CHEMISTRY
A EUROPEAN JOURNAL

DOI: 10.1002/chem.200601757

[3.3]Ferrocenophanes with Guanidine Bridging Units as Multisignalling Receptor Molecules for Selective Recognition of Anions, Cations, and Amino Acids

Francisco Otón,[a] Arturo Espinosa,[a] Alberto Tárraga,*[a] Carmen Ramírez de Arellano,[b] and Pedro Molina*[a]

Abstract: The synthesis, electrochemical, and optical properties of a new [3.3]ferrocenophane framework in which two ferrocene subunits, with similar electronic environments, are linked through two substituted guanidine moieties, are reported. The receptors **4**–**7** have been prepared in good yields by the reaction of bis(carbodiimide) **3** with primary amines. This architecture is exceptionally "tunable" because a variety of "legs" may be appended to the basic [3.3]ferrocenophane scaffold to give a wide range of signaling units. These receptors show remarkable ion-sensing properties, due to the presence of a redox active unit (ferrocene), and an amphoteric binding site (guanidine). In this nitrogen-rich structural motif the guanidine bridges act as multipoint binding sites for anions, cations, and amino acids. Sensing of anions takes place both by unprecedented redox-ratiometric measurements (F^-, Cl^-, AcO^-, NO_3^-, HSO_4^-, $H_2PO_4^-$, and $HP_2O_7^{3-}$), and colorimetric change (F^-, AcO^-, $H_2PO_4^-$, and $HP_2O_7^{3-}$). Sensing and discrimination of amino acids takes place by redox-ratiometric measurements, whereas the recognition of metal cations (Zn^{2+}, Ni^{2+}, and Cd^{2+}) is achieved either by electrochemical or fluorescence measurements. Moreover, the reported receptors display splitting of the oxidation wave of the Fe^{II}/Fe^{III} redox couple, and form the mixed-valence species $\mathbf{4}^{+\cdot}$-$\mathbf{7}^{+\cdot}$ by electrochemical partial oxidation which, interestingly, show intervalence charge-transfer transitions associated to the appearance of absorption bands in the near infrared spectral region.

Keywords: amino acids · ferrocene · guanidine · mixed-valence compounds · molecular recognition

Introduction

The development of chemosensors capable of recognizing and sensing anions and cations is one of the most challenging fields from the viewpoint of organic and supramolecular chemistry. These multisite ligands, which are able to bind a single heteroditopic guest, or simultaneously bind to a non-identical guest, have been achieved by integrating cationic and anionic guest binding sites in a single molecule.[1]

The guanidine function, due to its amphoteric nature, has a rich history in biological[2] and artificial receptors.[3] The guanidinium group within a variety of molecular architectures forms strong noncovalent interactions with anionic groups through hydrogen-bonding and charge-pairing interactions. In addition, deprotonated guanidines (guanidinates) have the potential to develop into valuable ancillary ligands in coordination and organometallic chemistry,[4] although the straightforward coordination of neutral guanidines to metal centers remains comparatively underdeveloped,[5] and metal-guanidinyl complexes are barely known and unexplored.[6]

Ferrocene-based ligands have been found to be useful for incorporating redox functions into supramolecular complexes that bind and allow the electrochemical sensing of cations,[7] anions,[8] and neutral molecules[9] by a change in the oxidation potential of the ferrocene. Despite the rich chemistry of guanidines, as the binding site, and ferrocene,

[a] F. Otón, Dr. A. Espinosa, Prof. A. Tárraga, Prof. P. Molina
Universidad de Murcia
Departamento de Química Orgánica, Facultad de Química
Campus de Espinardo 30100 Murcia (Spain)
Fax: (+34) 968-364-149
E-mail: atarraga@um.es
pmolina@um.es

[b] Dr. C. R. de Arellano
Universidad de Valencia
Departamento de Química Orgánica, Facultad de Farmacia
Campus de Burjasot, 46100 Valencia (Spain)

Supporting information for this article is available on the WWW under http://www.chemeurj.org/ or from the author.

as the redox signaling unit, only one example of a guanidinyl–ferrocene ligand has been described .[10]

With these considerations in mind, we decided to combine the redox activity of the ferrocene group with the binding ability of the guanidine group in a highly preorganized system. Here, we report a set of extremely nitrogen-rich [3.3]ferrocenophanes in which the two ferrocene subunits have similar electronic environments and are linked by two naphthyl-, (substituted) phenyl-, ferrocenyl-, or pyridyl-appended guanidine moieties. The presence of multiple binding sites in the design of new structural motifs, the multiresponsive character of the receptors, and the ability of the double-bridge to act as a favorable binding site for anions and cations in the recognition event are most noteworthy, allowing their use as multisignaling ion chemosensors.

Results and Discussion

Synthesis: Receptors **4–7** were prepared from 1,3,10,12-tetraaza[3.3]ferrocenophane **3** and the corresponding amine (Scheme 1). The aza-Wittig protocol[11] was the method of choice for building up the carbodiimide moieties in **3**, so that a reliable procedure for the synthesis of the bis(iminophosphorane) **2** was needed.[12] This compound was readily prepared by using the Staudinger reaction between triphenylphosphine and 1,1′-diazidoferrocene **1**,[13] which was prepared from ferrocene by using 2,4,6-triisopropylbenzenesulfonyl azide (trisyl azide) as a strong azide-transfer reagent. Thus, reaction of 1,1′-dilithioferrocene with trisyl azide at 0 °C afforded directly **1**, which was used without further purification for the next step in the Staudinger reaction with triphenylphosphane. This procedure allowed the one-pot conversion of ferrocene into bis(iminophosphorane) **2** in an overall yield of 59 %. The aza-Wittig reaction of **2** with 1,1′-bis(isocyanato)ferrocene[14] directly gave the bis(carbodiimide) **3** as the only reaction product and in 88 % yield,[15] which was fully characterized by using the standard spectroscopic procedures. It is worth mentioning that whilst its ^{1}H NMR spectrum shows two different pseudo-triplets, corresponding to the H_α and H_β present in the Cp units belonging to the ferrocene moieties, the ^{13}C NMR shows only one signal at $\delta = 66.29$ ppm for the corresponding C_α and C_β, which was confirmed by using HMQC experiments. Receptors **4–7** were prepared in yields ranging from 70 to 82 % from **3** and 4-methylbenzylamine, 1-aminomethylnaphthalene, 2-(2-aminoethylamino)-5-nitropyridine, or ferrocenylmethylamine,[16] respectively(Scheme 1). Elemental analysis and ^{1}H, ^{13}C NMR, and mass spectra were consistent with the proposed structures for these receptors.

Structure determination: The crystal structure of compound **7**·DMSO was determined by single-crystal X-ray diffraction (Figure 1). The structure shows four ferrocenyl units connected by two guanidine moieties. The molecule consists of a [-Fe-Cp-N=C-NH-Cp-]$_2$ cycle containing two ferrocenyl bridging units (Fe1 and Fe2) and two exocyclic -NH-CH$_2$-CpFeCp fragments. The ferrocenyl units in the cycle are perpendicular to each other with an Fe1···Fe2 distance of 5.993 Å (86.2° Cp-Fe1-Cp and Cp-Fe2-Cp lines angle). The guanidine moieties, which make a 49.9° dihedral angle, present both an endocyclic and an exocyclic N–H group. One of the endocyclic N–H groups forms an intramolecular N–H···N=C hydrogen bond (N4···N2 3.053(5), H4···N2 2.24(2) Å, N4–H4···N2 155(4)°) thus, connecting both guanidine groups and constraining the ferrocenophane cavity. The remaining endocyclic N–H group forms an N–H···O=S hydrogen bond with an exocyclic solvated dimethyl sulfoxide unit (N1···O1 2.929(5), H1···O1 2.062(17) Å,

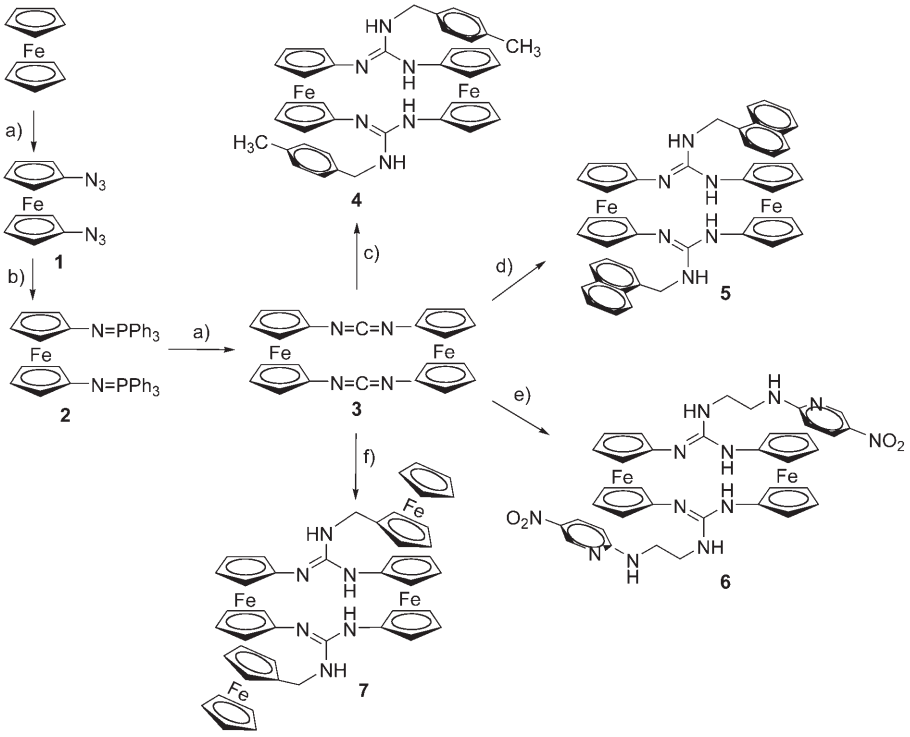

Scheme 1. Synthesis of [3,3]ferrocenophanes **3–7;** a) i) *n*BuLi, diethyl ether, RT, 16 h; ii) trisylazide, diethyl ether, 0 °C→RT, 4 h; 62 %; b) PPh_3, CH_2Cl_2, RT, 2.5 h, 92 %; c) 1,1′bis(isocyanato)ferrocene, dry THF, RT, N_2, 1 h, 88 %; d) 4-methylbenzylamine, dry THF, RT, 3 h, 77 %; e) 1-aminomethylnaphthalene, dry THF, RT, 3 h, 75 %; f) 2-(2-aminoethylamino)-5-nitropyridine, dry THF, RT, 3 h, 82 %; g) 1-aminomethylferrocene, dry THF, RT, 3 h, 70 %.

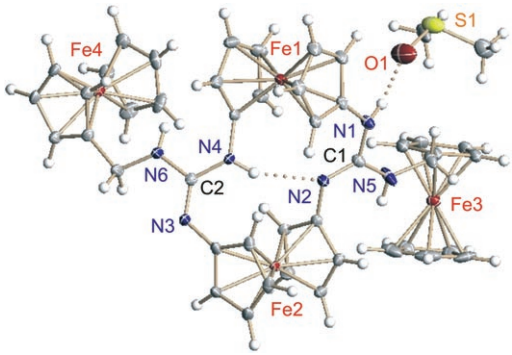

Figure 1. Ellipsoid plot of the molecular structure of receptor **7**, showing the atom labeling. Thermal ellipsoids are drawn at the 50% probability level.

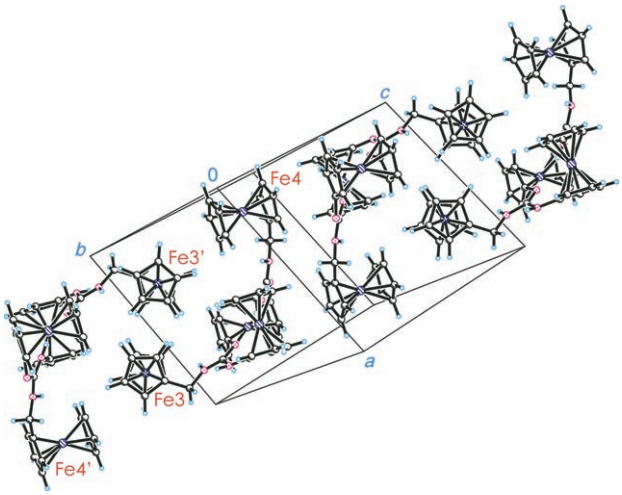

Figure 2. Crystal packing view of compound **7** showing the molecular ribbons.

N1−H1···O1 169(5)°). The constraint produced from the intramolecular N−H···N hydrogen bond, probably prevents the solvent inclusion. The position of the exocyclic N−H groups, located between an endocyclic and an exocyclic ferrocenyl group, seems to prevent them from acting as hydrogen bond donors. In the crystal, the exocyclic ferrocenyl fragments adopt a cisoid conformation (Figure 2). The molecules form molecular ribbons through herringbone-type interactions with parallel (Fe3···Fe3′) and perpendicular (Fe3···Fe4′) intermolecular ferrocenyl units at 5.723 and 6.401 Å, respectively.

Table 1. ΔE_p[a] values associated with the complexing processes between the free receptor R and the appropriate anion.

Compd	R[b]	$[R{\cdot}F]^-$	$[R{\cdot}HP_2O_7]^{3-}$	$[R{\cdot}OAc]^-$	$[R{\cdot}H_2PO_4]^-$	$[R{\cdot}HSO_4]^-$
4	−390	+10	+10	+10	+20	+110
	−110	–	–	–	−70	−20
5	−350	−10	−20	−10	+20	+90
	−90	–	–	–	−90	−20
6	−370	+10	−30	+10	+10	+130
	−120	–	–	–	−60	00
7[c]	−450	−30	−20	−20	−30	00
	−150	–	–	–	–	00
	+60	−90	−120	−60	−50	00

[a] In mV, resulting from the DPV experiments carried out in DMSO/H_2O (4:1). [b] E_p values corresponding to the free ligand in the same solvent. [c] Values obtained in a DMSO solution.

The DFT calculated geometry (see Figure S26 in the Supporting Information) for a model receptor **8**, which is similar to **4**–**7** but appended with methyl groups at the exocyclic guanidine positions, is in full agreement (Fe1···Fe2 6.097 Å; N2···N4 3.110 Å; N4−H4···N2 155.5°) with the above-mentioned experimental structure and has been used for the study of some binding properties described below.

Electrochemical sensing properties: At first the binding and recognition capability of receptors **4**–**7** towards various anions and cations were evaluated by differential pulse voltammetry (DPV).[17] The DPV results for receptors **4**–**6** in DMSO/H_2O (4:1, v/v) display two one-electron oxidation peaks in the range $E_p^1 = -390$ to -350 mV and $E_p^2 = -90$ to -120 mV versus Fe^{II}/Fe^{III} redox couple, whereas the DPV of receptor **7**, in DMSO, exhibits three well-resolved peaks: Two one-electron oxidation peaks at -440 and -150 mV and another one, with a potential at +50 mV versus Fe^{II}/Fe^{III} redox couple, which is actually due to two closely overlapping one-electron transfer processes corresponding to the oxidation of the peripheral ferrocenes (Table 1).

In contrast to most reported ferrocene-based redox sensors that rely on changes in the oxidation potential of the ferrocene, in the newly designed receptors not only the occurrence of two oxidation peaks, but also the magnitude of the ΔE_p (250–280 mV for receptors **4**–**6** and $\Delta E_p = 290$ and 200 mV, respectively, for receptor **7**) allow that in this structural motif the different perturbation of the two oxidation peaks, upon complexation, can be used for the first time as a redox-ratiometric measurement of the binding event.

Preliminary electrochemical studies with various anions (F^-, Cl^-, AcO^-, NO_3^-, HSO_4^-, $H_2PO_4^-$, and $HP_2O_7^{3-}$) in the form of the corresponding tetrabutylammonium salts, revealed a behavior that was quite different from the previous ferrocene-based anion receptors. Addition of increasing amounts of F^-, AcO^-, and $HP_2O_7^{3-}$ ions to a solution of receptors **4**–**6** in DMSO/H_2O, caused the complete disappearance of the second oxidation peak whereas the first oxidation peak was apparently not perturbed. The interaction between the F^- ion and the model receptor **8** was modeled by DFT calculations. The resulting $[\mathbf{8}{\cdot}F]^-$ complex (Figure 3), for which a free energy of complexation of -2.52 kcal mol^{-1}

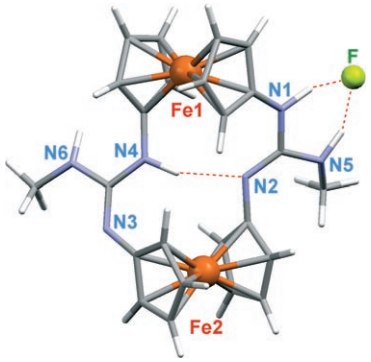

Figure 3. Calculated (B3LYP/aug6-31G*) structure for the [**8**·F]$^-$ complex.

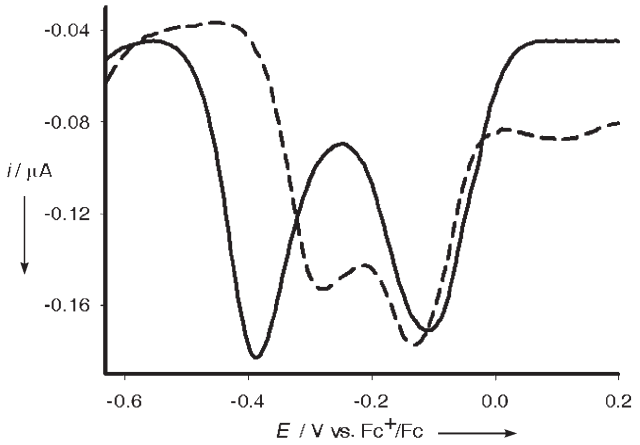

Figure 4. Evolution of the DPV of **4** (1 mM) in DMSO/H_2O (4:1) by using $[(n\text{Bu})_4\text{N}]PF_6$ (0.1 M) as supporting electrolyte, scanned at 4 mV s^{-1}, from −0.6 V to 0.2 V, when 0 (——) and 3.5 (– – –) equiv of HSO_4^- is added.

was calculated in DMSO solution, is formed upon rotation of the exocyclic −$NHCH_3$ group belonging to the guanidine bridge acting as acceptor in the intramolecular hydrogen bond (dihedral N1-C1-N5-H angle −5.9°; 174.4° in **8**). The two N−H groups in this guanidine moiety form a six-membered chelate ring with the F^- ion (N1H1···F 1.518 Å; N5−H5···F 1.710 Å). Taking into account that the geometry optimization was performed in the gas phase, the rather long N1−H1 bond (1.071 Å) actually means that N1 is deprotonated, causing a considerable increase of electron density both at N2, thus strengthening the intramolecular hydrogen bond (N4−H4···N2 2.075 Å; 2.153 Å in **8**) (see Table S5 in the Supporting Information), and at Fe1, which therefore becomes more easily oxidized (cathodic shift of the second oxidation peak up to the value of the first oxidation process).

On the other hand, the addition of $H_2PO_4^-$ and HSO_4^- elicited different electrochemical responses. On stepwise addition of $H_2PO_4^-$, the first oxidation peaks were slightly shifted anodically by +10–+20 mV, whereas the second oxidation peaks were remarkably shifted cathodically by −60 to −90 mV. In contrast, in the presence of the HSO_4^- ion the first oxidation peaks were dramatically shifted anodically by +90 to +130 mV, whereas the second oxidation peaks were slightly shifted cathodically by −20 mV in the case of **4** (Figure 4) and **5**, whereas in **6** they remained unaltered. The presence of Cl^- and NO_3^- ions had no effect on the DPV, even when present in large excess (see Figure S2, S3, S6, S7, S10, and S12 in the Supporting Information). Examining the relative perturbations at the two oxidation peaks upon the addition of these guest anions yields two interesting conclusions; a) $H_2PO_4^-$ causes a large relative perturbation at the second oxidation peaks, whereas HSO_4^- interacts more strongly close to the unit responsible of the first oxidation peaks and; b) the observation of anodic shifts in the first oxidation peaks, contrasts with previous examples of the binding of these oxoanions by ferrocene receptors where guests have been sensed through cathodic shifts in potential. Taking into account that HSO_4^- is considerably more acidic than $H_2PO_4^-$, and that the anodic shift of the first oxidation peaks is higher for the HSO_4^- ion than for $H_2PO_4^-$ anion, the observed electrochemical behavior is consistent with a guest-to-host proton-transfer reaction (anodic shift of the first oxidation peaks) accompanied by hydrogen-bond formation and subsequent anion coordination (cathodic shift of the second oxidation peaks).[18] A modeling of the host–guest interaction in the case of the HSO_4^- ion with the model receptor **8** yielded the structure of the [**8**·HSO_4]$^-$ complex displayed in Figure 5 (calculated free energy of

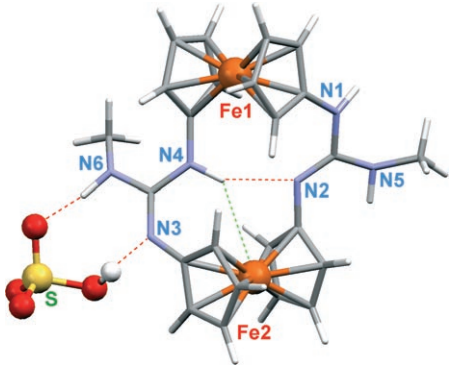

Figure 5. Calculated (B3LYP/aug6-31G*) structure for the [**8**·HSO_4]$^-$ complex.

complexation in DMSO solution −2.40 Kcal mol^{-1}). After rotation of the exocyclic −$NHCH_3$ group (dihedral angle N3-C2-N6-H 1.5°; −156.9° in **8**) at the guanidine bridge acting as intramolecular hydrogen bond donor, the latter is weakened (N4H4···N2 2.171 Å; 2.153 Å in **8**) as a consequence of the complementary interaction with the anion (OH···N3 1.900 Å; O···H6N6 1.817 Å), and increases the interaction of the internal H4 atom with the basic Fe2 center (H4···Fe2 2.986 Å; 3.029 Å in **8**) (see Table S5 in the Supporting Information for more details of geometry) which, therefore, becomes more difficult to oxidize (anodic shift of the first oxidation peak). On the contrary, when the binding ability of host **8** towards the $H_2PO_4^-$ ion was checked, the

calculated most stable complex was not that resulting from protonation at N3, like $[\mathbf{8}\cdot HSO_4]^-$ (Figure 5), but that promoting deprotonation at N1, like $[\mathbf{8}\cdot F]^-$ (Figure 3). The host–guest interaction in $[\mathbf{8}\cdot H_2PO_4]^-$ (See Figure S27 in the Supporting Information) is held by the formation of an eight-membered chelate ring with two almost linear hydrogen bonds (N1–H1···O 1.031 and 1.837 Å, 170.9°; N5–H5···O 1.026 and 1.913 Å, 162.1°), which yields an overall free energy of complexation in DMSO of −0.88 kcal mol^{-1}.

Addition of F^-, AcO^-, $H_2PO_4^-$, and $HP_2O_7^{3-}$ ions to a solution of the receptor **7** in DMSO induced the complete disappearance of the second oxidation peak, whereas the first and third oxidation peaks were shifted cathodically, such a shift being higher for the third oxidation peak than for the first one. Interestingly, the presence of the HSO_4^- ion had no effect on the DPV, even when present in large excess (Table 1).

The DPV results for the receptors **4** and **5** in CH_2Cl_2 show two well-spaced ($\Delta E_p = 460$ and 410 mV, respectively) reversible one-electron oxidations peaks: The first one at −480 and −440 mV and the second one at −20 and −30 mV, respectively, versus Fe^{II}/Fe^{III} redox couple. Upon protonation by the addition of one equivalent of HBF_4 in acetonitrile, the redox peaks were shifted anodically by −70 and −20 mV, and by 270 and 240 mV, respectively ($\Delta E_p =$ 340 mV and 260 mV, respectively). These guanidinium receptors $\mathbf{4}\cdot H^+$ and $\mathbf{5}\cdot H^+$ have also been used to investigate its ability to electrochemically sense anion binding. Upon addition of F^-, AcO^-, HSO_4^-, $H_2PO_4^-$, and $HP_2O_7^{3-}$ anions two new redox peaks evolved, which were shifted cathodically. The evolving peaks appeared at virtually the same potential as that of the free guanidine receptors, indicating that a deprotonation has taken place. A control experiment with the addition of K_2CO_3/H_2O to the final solution, which caused no further change in the redox behavior, showed that this response was equivalent to deprotonation.

However, the addition of NO_3^- and Cl^- elicited a different electrochemical response. In both cases the two redox peaks are shifted cathodically to −90 and −50 mV, and to −200 and −120 mV, respectively, for NO_3^- (Figure 6), and to −80 and −130, or 100 mV, respectively, for Cl^- (see Figure S4 and S8 in the Supporting Information). These findings are indicative that oxidation is facilitated by the proximate coordination of the anion to the guanidinium moiety, and underscore the selectivity of the guanidinium receptors $\mathbf{4}\cdot H^+$ and $\mathbf{5}\cdot H^+$ for NO_3^- and Cl^- ions in CH_2Cl_2, the electrochemical changes being higher for the NO_3^- ion than for the Cl^- ion (Table 2). One of the current challenges in anion-recognition chemistry involves the preparation of receptors that show high HSO_4^-/NO_3^- selectivity,[19] and one attractive feature of this new guanidino-ferrocenophane structural motif is its ability to bind selectively HSO_4^- in the presence of NO_3^- ion.

The development of artificial receptors for amino acids is slow due to their hydrophilicity and bifunctional character. To our knowledge, there is only one example of a ferrocene-based redox receptor for amino acids,[20] which involves a ferrocene with two open arms bearing multipoint binding sites.

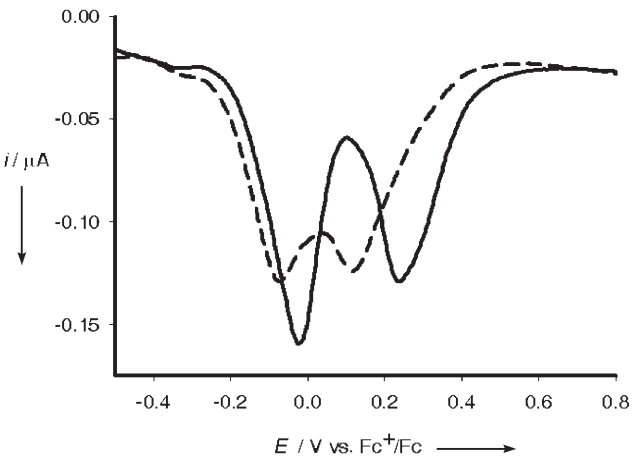

Figure 6. Evolution of the DPV of $\mathbf{5}\cdot H^+$ (1 mM) in CH_2Cl_2 by using $[(n\text{Bu})_4N]PF_6$ (0.1 M) as supporting electrolyte, scanned at 4 mV s^{-1}, from −0.5 V to 0.8 V, when 0 (——) and 9 (– – –) equiv of NO_3^- is added.

Table 2. ΔE_p[a] values associated with the complexation processes between the protonated receptor $[R\cdot H]^+$ and the appropriate anion.

Compd	R[b]	$[RH]^+$[c]	$[RH\cdot NO_3]$	[RH·Cl]
4	−480	−70	−90	−80
	−20	+270	−200	−130
5	−440	−20	−50	−80
	−30	+240	−120	−100

[a] In mV, resulting from the DPV experiments carried out in CH_2Cl_2. [b] E_p values in mV corresponding to the free receptor in CH_2Cl_2. [c] E_p values in mV corresponding to the protonated receptor in CH_2Cl_2.

To assess how these receptors might act in a sensing capacity, the binding between L-Glu, L-Trp, L-Leu, and L-Phe ($DMSO/H_2O$ 9:1, v/v; $c = 2.5\times10^{-2}$ M; pH 7.2–9.2) and receptors **4** and **5** (CH_2Cl_2/CH_3CN 3:2, v/v; $c = 1\times10^{-3}$ M) were followed by DPV. Significantly, the addition of 0.5 equivalents of L-Glu, or L-Trp to a solution of the receptor **4** or **5** brought about the disappearance of the second oxidation peak and no change in the first oxidation peak was observed, as the AcO^- ion does. Interestingly, the addition of one equivalent of L-Leu or L-Phe brought about significant cathodic shifts of both oxidation peaks (Table 3 and Figure 7), in line with the results on the binding of NO_3^- and Cl^- anions by the protonated receptors $\mathbf{4}\cdot H^+$ and $\mathbf{5}\cdot H^+$ (see Figure S14 and S15 in the Supporting Information).

Table 3. ΔE_p[a] values associated with the complexation processes between the free receptor (R) and the appropriate amino acid

Compd	R[b]	L-Glu	L-Tryp	L-Leu	L-Phe
4	−470	+10	+10	00	−10
	−50	–	–	−40	−50
5	−430	+10	00	−40	−30
	−10	–	–	−70	−50

[a] In mV, resulting from the DPV experiments carried out in CH_2Cl_2/CH_3CN (3:2). [b] E_p values in mV corresponding to the free receptor in the same solvent.

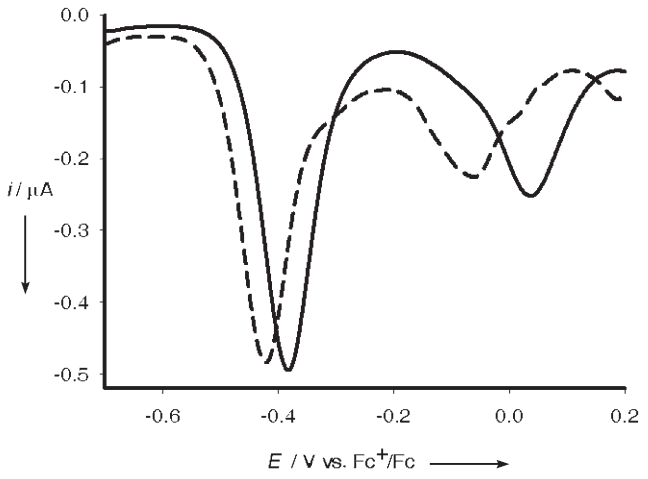

Figure 7. Evolution of the DPV of **5** (1 mM) in CH_2Cl_2/CH_3CN (3:2) by using $[(n\text{Bu})_4\text{N}]PF_6$ (0.1 M) as supporting electrolyte, scanned at 4 $mV\,s^{-1}$, from −0.7 V to 0.2 V, when 0 (——) and 1 (– – –) equiv of L-Leu is added.

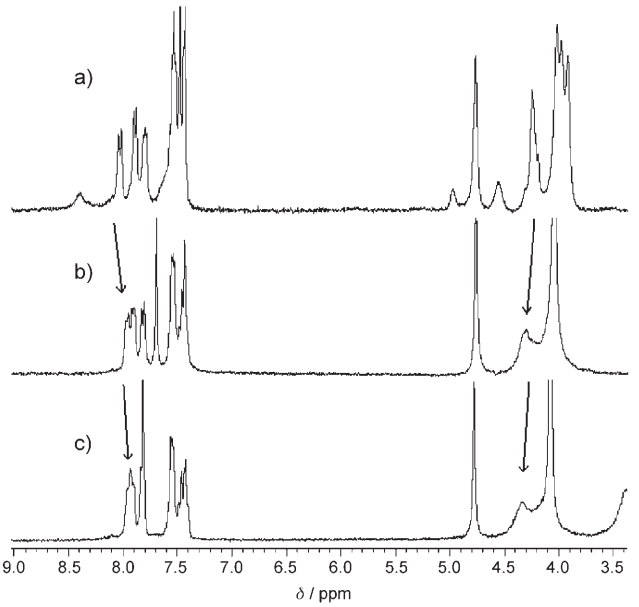

Figure 8. Evolution of the ^{1}H NMR spectra of **5** in CD_2Cl_2/CD_3CN (3:2) ($c = 5\times10^{-3}$ M) upon addition of increasing amounts of a solution of L-Glu 0.1 M in $[D_6]DMSO/D_2O$ (9:1): (a) **5**; (b) **5**+0.8 equiv; (c) **5**+1.6 equiv.

It is important to underline that in all the cases studied, the addition of the appropriate amino acid to the free receptor R promotes the total disappearance of the signals corresponding to the guanidine NH protons in the ^{1}H NMR spectrum, whereas the four signals due to the ferrocene moieties are strongly affected, giving rise to two different multiplets centered at $\delta = 4.33$ (4H) and 4.07 ppm (12H), respectively. It is worth mentioning that only in the case of the addition of glutamic acid an additional chemical shift change, corresponding to the H_8 proton within the naphthalene moiety, was also observed and as a consequence the binding constant of **5** and L-Glu was determined by a titration method by using ^{1}H NMR spectroscopy. Thus, addition of increasing amounts of a solution of L-Glu (in $[D_6]DMSO/D_2O$ 9:1) to a solution of compound **5** in CD_2Cl_2/CD_3CN (3:2) led to a significant high-field shift ($\Delta\delta = -0.11$ ppm) for the abovementioned H_8 proton (Figure 8). By using the computer program Wineqnmr[21] a $K_{as} = 5.2\times10^3\ M^{-1}$ (error < 10%) was calculated.

One of the most important attributes of receptors **4**–**7** was the presence of two ferrocene moieties in proximity to the cation-binding guanidine groups. Therefore, the metal recognition properties towards Li^+, Na^+, K^+, Mg^{2+}, Ca^{2+}, Ni^{2+}, Cd^{2+}, and Zn^{2+} metal ions were evaluated by electrochemical analysis. In $DMSO/CH_2Cl_2$ (3:2, v/v), no perturbation of the DPV voltammogram of **4**–**7** were observed upon addition of Li^+, Na^+, K^+, Mg^{2+}, Ca^{2+}, Ni^{2+}, and Cd^{2+} metal ions. However, upon addition of Zn^{2+} ions to receptors **4**–**6** a dramatic decrease in intensity of the first oxidation peak and no perturbation of the second oxidation peak was observed. Likewise, for receptor **7** the first oxidation peak disappeared whereas the second and third peaks remained unchanged (see Figure S16 in the Supporting Information).

These electrochemical results clearly revealed the advantage of the guanidino-ferrocenophane receptors **4**–**7** over the widely studied ferrocene-based receptors in which the presence of only one redox peak does not allow a dual redox peak ratiometric measurement upon a cationic or anionic recognition process. Isothermal titration calorimetry (ITC) provides useful insight into the nature of the binding interactions, and advantages of this method for studying anion recognition properties have been recently reported.[22] ITC experiments were carried out by adding aliquots of the appropriate anion ($c = 1.4\times10^{-2}$ M) to a solution of the adequate receptor ($c = 1\times10^{-3}$ M) at 298 K in DMSO. The association constants (K_{as}) were calculated by nonlinear least-squares analysis (Table 4). It should be noted that, as yet,

Table 4. ITC data[a] obtained from the titration experiments between the appropriate receptors and anions.

Receptor	Anion	K_{as}	R/A[b]	ΔH[c]	ΔS[d]
4	F^-	$4.6\times10^6\ M^{-1}$	1:1	−2370	22.5
		$4.9\times10^4\ M^{-2}$	1:2	−910	18.4
	AcO^-	$9.3\times10^3\ M^{-2}$	2:1	−1000	14.8
	$H_2PO_4^-$	$7.3\times10^3\ M^{-1}$	1:1	400	19.0
5	F^-	$1.4\times10^6\ M^{-2}$	2:1	−3450	16.5
		$2.7\times10^5\ M^{-1}$	1:1	−1150	21.0
	AcO^-	$5.2\times10^4\ M^{-2}$	2:1	2260	29.2
	$H_2PO_4^-$	$2.8\times10^4\ M^{-2}$	2:1	1600	25.7
6	F^-	$3.7\times10^4\ M^{-1}$	1:1	−3230	10.1
	$HP_2O_7^{3-}$	$1.8\times10^6\ M^{-2}$	2:1	−10050	−5.0
		$4.1\times10^4\ M^{-1}$	1:1	−2910	11.4
7	F^-	$2.3\times10^4\ M^{-1}$	1:1	−3470	8.4
	AcO^-	$1.8\times10^4\ M^{-2}$	2:1	−430	18.0
	$H_2PO_4^-$	$2.8\times10^4\ M^{-2}$	2:1	−3270	9.4
	$HP_2O_7^{3-}$	$8.9\times10^3\ M^{-2}$	2:1	3520	29.9

[a] All titrations were carried out in DMSO as solvent. [b] Stoichiometry receptor/anion (R/A). [c] $cal\,mol^{-1}$; the corresponding errors are given in the Supporting Information within the appropriate figure. [d] These values ($cal\,mol^{-1}\,K^{-1}$) are given directly by the software package supplied by MicroCal, and are included in the Supporting Information.

we have been unable to obtain reliable K_{as} values for the HSO_4^- ion binding by ITC under the conditions used for the other anions. On the other hand, when the Zn^{2+} ion was added to a solution of the receptors in DMSO/CH_2Cl_2 (3:2, v/v) the titration curves showed an inflection point around 0.5 equivalents of cation added, which evidenced the formation of 2:1 complexes. The association constants (K_{as}) were found to be $3.0\times10^4\,M^{-2}$ $4.2\times10^4\,M^{-2}$, $3.3\times10^4\,M^{-2}$, and $5.1\times10^4\,M^{-2}$ for **4**, **5**, **6**, and **7**, respectively (see Figure S17–S20 in the Supporting Information).

Several trends have emerged from the electrochemical study. First, neutral receptors **4**–**7** are able to recognize and discriminate not only F^-, AcO^-, HSO_4^-, $H_2PO_4^-$, and $HP_2O_7^{3-}$ ions, but also amino acids by using different variations of the two redox signals, in relatively polar solvent (DMSO/H_2O) where hydrogen-bonding interactions between the guanidine functional groups and the anions are usually weakened by competing solvent molecules. Second, the guanidinium receptors **4**·H^+ and **5**·H^+ selectively sense NO_3^- and Cl^- ions in a less polar solvent. Third, these receptors are also selective redox chemosensors of Zn^{2+} ions. These findings underscore an unreported redox-ratiometric behavior to sense anions, and amino acids which, in some cases, can be modulated in by simple protonation of the neutral receptors.

Colorimetric anion-sensing: The UV/Vis data obtained in CH_2Cl_2 for the new synthesized bisguanidyl ferrocenophane receptors **4**–**7** are consistent with most ferrocenyl chromophores in that they exhibit two charge-transfer bands in the visible region.[23] These spectra contain a prominent absorption band with a maximum at 363 nm, which can safely be ascribed to ligand-centered π–π* electronic transitions (L–π*). In addition to this band, another weaker absorption is detected at 443 nm, for **4**, **5**, and **7**, whereas in ligand **6** it is masked by the strong absorption bands. This weak absorption is produced either by two nearly degenerate transitions: An Fe^{II} d–d transition[24] or by a metal–ligand charge transfer (MLCT) process (d_π–π*). This assignment is in accordance with the latest theoretical treatment (model III) reported by Barlow and co-workers.[25]

Previous studies on ferrocene-based ligands have shown that their characteristic low-energy bands in the absorption spectra are perturbed by complexation.[26] Therefore, the anion recognition properties of these bisferrocene ligands, in CH_2Cl_2, towards F^-, Cl^-, AcO^-, NO_3^-, HSO_4^-, $H_2PO_4^-$, and $HP_2O_7^{3-}$ anions were also evaluated by UV/Vis spectroscopy. It is worth mentioning that no changes were observed in the UV/Vis spectra of receptors **4**, **5**, and **7** upon addition of the above-mentioned anions, even in a large excess.

However, for receptor **6** ($c=5\times10^{-5}$ M, in CH_2Cl_2), the presence of F^-, AcO^-, $H_2PO_4^-$, and $HP_2O_7^{3-}$ ions, induced a red-shift of the low-energy band ($\Delta\lambda_{max}=9$–19 nm) and an important increase of their molar absorptivity. This new band is responsible for a change of color and can be used for the "naked-eye" detection of these anions (Figure 9). No changes in the UV/Vis spectrum of this receptor were observed upon addition of an excess of Cl^-, NO_3^-, and HSO_4^- ions. Titration experiments for CH_2Cl_2 solutions of receptor **6** ($c=5\times10^{-5}$ M) and the corresponding anions were performed and analyzed quantitatively.[27] In all cases where an optical response could be detected the observation of well-defined isosbestic points in the evolution of the UV/Vis spectra, clearly indicates that a clean complexation equilibrium occurs. Titration data analysis gave the stability constants of 5.1×10^5 and $8.5\times10^5\,M^{-1}$ for $H_2PO_4^-$ and AcO^- ions, respectively, and confirmed the formation of 1:1 complex stoichiometries in solution.

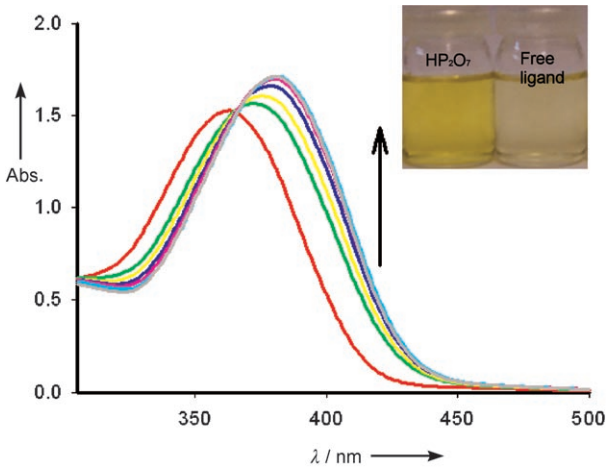

Figure 9. Changes in the absorption spectra of **6** ($c=5\times10^{-5}$ M in CH_2Cl_2) upon addition of increasing mounts of $HP_2O_7^{3-}$. The arrow indicates absorption that increases during the experiment. Onset: Change in the color of the receptor **6** upon addition of $HP_2O_7^{3-}$.

Fluorescence ion-sensing: The design of ferrocene-containing luminescent molecules may seem something of a contradiction in that ferrocene has been widely used as an emission quencher in intramolecular processes taking place in solution.[28] Recently, ferrocene has been advantageously used as a redox center to provide multiresponsive photo- and electrochemically active compounds.[29] The absorption spectrum of receptor **5** shows an intense band at 283 nm attributed to the naphthalene units along with a very weak band at low energy centered at 443 nm, which can safely be ascribed to the metal-to-ligand charge transfer (LMCT) transition in the ferrocene moieties. So, as it was expected, receptor **5** displays a very weak fluorescence. The emission spectrum ($\lambda_{exc}=310$ nm) exhibits a structureless band centered at 354 nm, due to the naphthalene monomer emission. Upon addition of small amounts of Zn^{2+} to the solution of receptor **5** in dichloromethane ($c=5\times10^{-5}$ M), a pronounced red-shift of 30 nm along with an intensity increase of the naphthalene monomer emission was observed (Figure 10). The final fluorescence-increase factor (FEF) was five and the quantum yield ($\Phi=0.070$) resulted in a fourfold increase compared to that of the free receptor ($\Phi=0.016$). The stoichiometry of the complex was determined by fluorogenic titration, and the results obtained indicate the formation of a

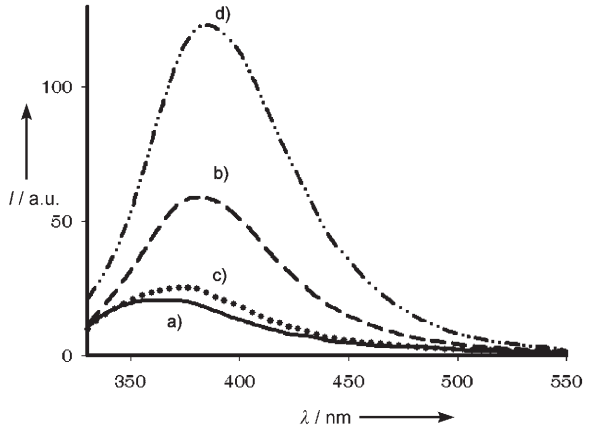

Figure 10. Changes in the fluorescence emission spectra of **5**: a) (λ_{exc} = 310 nm, ——) in CH_2Cl_2 ($c = 5\times10^{-5}$ M), upon titration with: b) HBF_4 (1 equiv, – – –) and; (d) Zn^{2+} cation (4.5 equiv, –•–•). c) Spectrum (•••••) corresponds to the complex formed between $[\mathbf{5}\cdot H]^+$ and the NO_3^- ion (1.6 equiv).

2:1 complex giving an association constant (K_{as}) of 5×10^4 M^{-2}. Similar results were obtained in the presence of Ni^{2+} ($\Phi = 0.063$; FEF = 4; 2:1 complex stoichiometry and $K_{as} = 5.5\times10^4$ M^{-2}), and Cd^{2+} ($\Phi = 0.092$; FEF = 6; 2:1 complex stoichiometry and $K_{as} = 2.4\times10^4$ M^{-2}) metal ions.

Interestingly, the addition of one equivalent of HBF_4 also produced an intensity increase in the naphthalene emission albeit lower ($\Phi = 0.043$ versus 0.016) than that originated by the abovementioned metal ions. Remarkably, stepwise addition of NO_3^- anion to a solution of $\mathbf{5}\cdot H^+$ produced quenching of the emission ($\Phi = 0.020$), whereas addition of AcO^-, HSO_4^-, and $H_2PO_4^-$ ions, clearly induced deprotonation. Fluorogenic titration with NO_3^- ion indicates the formation of a 1:1 complex giving a $K_{as} = 2.6\times10^6$ M^{-1} (see Figure S23 and S24 in the Supporting Information).

Spectroelectrochemical studies: The thermodynamic stability of the mixed-valence species $\mathbf{4}^{+\bullet}$–$\mathbf{7}^{+\bullet}$ were initially estimated from the comproportionation constants K_c which were calculated[30] from the observed wave-splitting. Free energies of comproportionation, $\Delta G_c^{\ominus}$, from 8.25 kcal mol^{-1} (2887 cm^{-1}) to 10.47 kcal mol^{-1} (3662 cm^{-1}) were obtained the resulting values of K_c (1.1×10^6 to 4.7×10^7). The $\Delta E_{1/2}$ (and $\Delta G_c^{\ominus}$) value may be used for the assessment of the extent of ferrocenyl–ferrocenyl coupling although it only provides a crude estimation of such an interaction because this magnitude has been shown to be extremely medium-dependent[31] and contains additional contributions that are difficult to estimate for delocalized systems. The stability of $\mathbf{4}^{+\bullet}$–$\mathbf{7}^{+\bullet}$ in CH_2Cl_2 solution should allow the detection of an intervalence charge-transfer (IVCT) band in the near-IR spectral region.[32] The generation of the oxidized species $\mathbf{4}^{+\bullet}$–$\mathbf{7}^{+\bullet}$ was performed electrochemically and monitored by absorption spectroscopy. Stepwise coulometric titrations were performed on approximately 3.5×10^{-3} mol L^{-1} solutions of these complexes in CH_2Cl_2, with $[(n\text{Bu})_4\text{N}]PF_6$ (0.15 M) as supporting electrolyte. Generation of the monooxidized species was performed by constant potential electrolysis, 0.14 V above $E_{1/2}$ of the first oxidation peak. The most interesting feature is that during the oxidation of **4**–**7** a new weak and broad band, centered at $\nu_{max} = 10296$–10438 cm^{-1} ($\lambda_{max} = 958$–971 nm, $\varepsilon = 324$–587 M^{-1} cm^{-1}) continuously increasing until one electron is removed (see Tables S3 and S4 and Figure S25 in the Supporting Information). Along with the change of this band, the appearance and maintenance of well-defined isosbestic points are observed. Interestingly, on removing more electrons ($1 \le n \le 2$) at a constant potential of 0.20 V, the intensity of this band decreases until it disappears when the dication $\mathbf{4}^{2+}$-$\mathbf{7}^{2+}$ is completely formed, which confirms the IVCT character of this band (Figure 11). Furthermore, the band is in the anticipated spectral region, judging from previously reported IVCT transitions in other dinuclear ferrocene compounds with good levels of electronic coupling.[32]

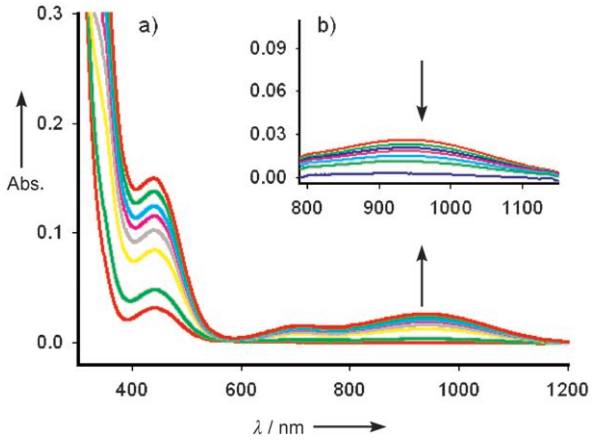

Figure 11. Evolution of UV/Vis/NIR spectra during the course of the oxidation of compound **5** in CH_2Cl_2 with $[(n\text{Bu})_4\text{N}]PF_6$ (0.15 M) as supporting electrolyte when: a) $0 \le n \le 1$, or b) $1 \le n \le 2$ electrons are removed. Arrows indicate absorptions that increase or decrease during the experiment.

The application of the two-state Hush model[33] to the spectra of the mixed-valence species $\mathbf{4}^{+\bullet}$–$\mathbf{7}^{+\bullet}$ predicts a half-height bandwidth ($\Delta\nu_{1/2}$) of $[(2311)\nu_{max}]^{1/2} = 4876$–$4910$ cm^{-1}, which is considerably larger than the values determined experimentally ($\Delta\nu_{1/2} = 2493$–3136 cm^{-1}) from nonlinear least-squares Gaussian-fitting deconvolution of the reduced (ε/ν [L mol^{-1}] versus ν [cm^{-1}]) spectra. Because the Hush model can only be rigorously applied to weakly coupled mixed-valence species,[33–34] the overestimation of the $\Delta\nu_{1/2}$ and the large K_c values both indicate that electronic coupling in these systems is quite significant. Parameter Γ, determined from the experimental and predicted bandwidths, provides a useful criterion for determining whether a particular system is weakly coupled, moderately coupled, at the Class II–III transition, or strongly coupled (Class III).[35] Thus, the resulting values of $\Gamma = 0.36$–0.49 indicate that $\mathbf{4}^{+\bullet}$–$\mathbf{7}^{+\bullet}$ systems lie close to the transition between Class II and II–III classification for a mixed-valence compound.

These results are remarkable because the extent of electronic communication, as estimated by the difference between the two observed oxidation peaks, is quite pronounced. In comparison, [2.2]ferrocenophane-diyne shows a $\Delta E_{1/2}$ of 0.35 V[36] and [4.4]ferrocenophane-tetrayne a $\Delta E_{1/2}$ value of 0.25 V.[37] All these $\Delta E_{1/2}$ values are smaller than that measured for the herein reported nitrogen-rich [3.3]ferrocenophanes, which clearly illustrate for the first time an effective electronic coupling between two ferrocene units mediated by guanidine bridges.

Conclusion

We have designed new guanidino-ferrocene based receptors with multiproperties, which open the door to new types of redox-ratiometric chemosensors. This architecture is exceptionally "tunable" because a variety of "legs" may be appended to the basic [3.3]ferrocenophane scaffold to give a wide range of signaling units. They allow the sensing of not only the F^-, AcO^-, HSO_4^-, $H_2PO_4^-$, and $HP_2O_7^{3-}$ ions, but also the amino acids L-Glu, L-Trp, L-Leu, and L-Phe through two different oxidation peak perturbations, in a highly polar environment. Additionally, its monoprotonated form is able to selectively sense $Cl^-$and NO_3^- by redox-ratiometric measurements. These receptors are also selective redox chemosensors of Zn^{2+} cations and, due to the presence of the naphthalene ring, receptor **5** is able to act as fluorescent chemosensor of Zn^{2+}, Ni^{2+}, and Cd^{2+} metal cations. Furthermore, proton-induced complexation of **5** provides a versatile means of selectively sensing NO_3^- through fluorescence-emission quenching, whereas the presence of different nitrogen functionalities in receptor **6** allow the colorimetric sensing of F^-, AcO^-, $H_2PO_4^-$, and $HP_2O_7^{3-}$ anions. On the other hand, the extent of electronic communication in these nitrogen-rich [3.3]ferrocenophanes, as estimated both by the difference between the two observed oxidation peaks and from spectroelectrochemical experiments, is quite pronounced, which clearly illustrates for the first time an effective electronic coupling between two ferrocene units mediated by guanidine bridges. These unprecedented structural motifs pave the way to the design of a new generation of homoditopic receptors in which the ferrocene/ferrocenium redox couple and the ability of the guanidine moiety to act as a binding site, may operate cooperatively within the molecule. This synergistic relation may create molecular systems which can behave not only as redox-switching homotopic receptors, with the dual capability of selectively sensing anions and cations, but also as suitable models displaying charge-transfer transitions.

Experimental Section

All reactions were carried out by using solvents which were dried by routine procedures. All melting points were determined on a Kofler hotplate melting-point apparatus and are uncorrected. IR spectra were determined as Nujol emulsions or films on a Nicolet Impact 400 spectrophotometer. UV/Vis/NIR spectra were taken on a Varian Cary 5000 spectrophotometer. ^1H and ^{13}C NMR spectra were recorded on a Bruker AC200, 300, 400, or 600 MHz instrument. The following abbreviations for stating the multiplicity of the signals have been used: s (singlet), brs (broad singlet), d (doublet), t (triplet), brt (broad triplet), m (multiplet), and q (quaternary carbon atom). Chemical shifts refer to signals of tetramethylsilane in the case of ^1H and ^{13}C NMR spectra. The EI mass spectra were recorded on a Fisons AUTOSPEC 500 VG spectrometer. Microanalyses were performed on a Carlo-Erba 1108 instrument. Crystallographic measurements were made at 233(2) K on a Brücker diffractometer with the area-detector diffractometer positioned at the window of a rotating anode generator using MoK_α radiation (0.71073 Å). The cyclic voltammetric measurements were performed on a QUICELTRON potentiostat/galvanostat controlled by a personal computer and driven by dedicated software. Cyclic voltammetry was performed by using a conventional three-electrode configuration consisting of platinum working and auxiliary electrodes and a SCE reference electrode. The experiments were carried out by using a 10^{-3} M solution of sample in the appropriate solvent containing 0.1 M $[(n\text{Bu})_4\text{N}]PF_6$ as supporting electrolyte. Deoxygenation of the solutions was achieved by bubbling nitrogen for at least 10 min and the working electrode was cleaned after each run. The cyclic voltammograms were recorded with a scan rate increasing from 0.05 to 1.00 $V\,s^{-1}$. The DPV voltammograms were recorded in the appropriate solvent: $\Delta E_s = 4$ mV; $\Delta E_p = 25$ mV and $f = 15$ Hz. Ferrocene was used as an internal reference both for potential calibration and for reversibility criteria in all the solvents used. Oxidations were performed by electrolysis in a three-electrode cell under argon by using dry CH_2Cl_2 as a solvent and 0.15 M $[(n\text{Bu})_4\text{N}]PF_6$ as supporting electrolyte. The progress of the oxidation was followed coulometrically (or chronoamperometrically) by 263 A of a EG&PAR potentiostat-galvanostat. The reference electrode and the counter electrode were separately immersed in the solvent containing the supporting electrolyte and isolated from the bulk solution by a glass frit. The working electrode was a platinum grid. UV/Vis/Near IR absorption spectra were regularly recorded by transferring a small aliquot of the solution contained in the electrochemical cell into a UV quartz cell for a different average number of removed electrons. Microcalorimetric titrations were carried out by using an isothermal titration calorimeter (ITC). The ORIGIN software, provided by Microcal Inc. was used to calculate the binding constant. The titrations were performed as follows: A solution of the receptor in DMSO ($c = 1 \times 10^{-3}$ M) was prepared and was titrated with the appropriate alkylammonium salt at 25 °C. The original heat pulses were normalized by using reference titrations carried out with the same salt solution, but pure solvent, as opposed to the solution containing the receptor. Calculated geometries were fully optimized in the gas phase with tight convergence criteria at the DFT level with the Gaussian 03 package,[38] by using the B3LYP[39] functional and the 6-31G* basis set for all atoms, and adding diffuse functions on donor atoms (F, O, and N) (denoted as aug-6-31G*). Solvent (DMSO) effects were considered by using the Tomasi PCM (polarizable continuum model) formalism[40] and were computed as single-point calculations on the gas-phase-optimized geometries.

Preparation of 1,1′-bis(azido)ferrocene (1): *n*BuLi (17.5 mL, 28.2 mmol) and dry TMEDA (4.25 mL, 28.2 mmol) were added dropwise to a solution of ferrocene (2.5 g, 13.4 mmol) in dry diethyl ether (45 mL) at room temperature and under a nitrogen atmosphere. The reaction mixture was stirred for 18 h and the mixture was then cooled to 0 °C. Then a solution of trisyl azide (9.7 g, 39.6 mmol) was slowly added. The solution was stirred in the dark for 4 h and afterwards water (20 mL) was added. The reaction mixture was stirred for 10 min and, after addition of water (50 mL), was extracted with diethyl ether (2 × 50 mL). The organic layers were washed with water, dried over anhydrous $MgSO_4$ and were separated by chromatography on a silica gel column in the dark by using *n*-hexane/EtOAc (9.7:0.3, $R_f = 0.53$) to give a solid which was crystallized at −40 °C in *n*-hexane to give yellow crystals (2.22 g; 62 %). The melting point and spectroscopic data of the product are coincident with those reported in the literature for **1**.[13]

1,1′-Bis(*N*-trifenilfosforanilideneamino)ferrocene (2): To a solution of 1,1′-bis(azido)ferrocene (**1**; 1.0 g, 1.35 mmol) in dry CH_2Cl_2 (60 mL), a so-

lution of triphenylphosphane (2.93 g, 4.07 mmol) in the same solvent (35 mL) was added at room temperature and under nitrogen. The solution was stirred for 3 h at room temperature and the solvent was removed under vacuum. The residue was triturated with diethyl ether (50 mL) to give **2** as a deep red solid (2.52 g, 92 %), which was obtained pure enough to be used without further purification. M.p. 161–165 °C (decomp); ^{1}H NMR (200 MHz, $CDCl_3$, −55 °C, TMS): $\delta = 7.82$ (m, 12H; Ar), 7.49 (m, 18H; Ar), 3.24 (s, 4H; Fc), 2.95 ppm (s, 4H; Fc); ^{13}C NMR (50 MHz, $CDCl_3$, −55 °C, TMS): $\delta = 132.4$ (d, ^3J(C,P) = 9.1 Hz; Ar, CH_{meta}), 131.6 (Ar, CH_{para}), 129.5 (d, ^1J(C,P) = 97.2 Hz; Ar, q), 128.4 (d, ^2J(C,P) = 11.1 Hz; Ar, CH_{ortho}), 68.1 (CH, Fc), 66.1 ppm (CH, Fc); ^{31}P NMR (81 MHz, $CDCl_3$, −55 °C): $\delta = 8.52$ ppm; IR (CH_2Cl_2): $\tilde{\nu}_{max}$ = 3060, 2957, 2922, 2860, 1659, 1587, 1470, 1434, 1378, 1291, 1112 cm^{-1}; MS (FAB$^+$), *m*/*z* (%): 737 (100) [M^++1].

Preparation of 1,3,10,12-tetraza[3,3]ferrocenophane (3): To a solution of 1,1′-bis(isocyanato)ferrocene (0.2 g, 0.74 mmol) in dry THF (50 mL), a solution of 1,1′-bis(*N*-triphenylphosphoranylideneamino)ferrocene **2** (0.514 g, 0.74 mmol) in the same solvent (100 mL) was added at room temperature and under nitrogen atmosphere. The reaction mixture was stirred at room temperature for 1 h and the solvent was removed under reduced pressure. The resulting residue was crystallized from CH_2Cl_2/diethyl ether (3:2) to give **3** (0.275 g, 88 %). M.p. 175–178 °C (decomp); ^{1}H NMR (200 MHz, $CDCl_3$, 25 °C, TMS): $\delta = 4.32$ (t, ^3J(H,H) = 1.8 Hz, 8H; Fc), 4.18 ppm (t, ^3J(H,H) = 1.8 Hz, 8H; Fc); ^{13}C NMR (50 MHz, $CDCl_3$, 25 °C, TMS): $\delta = 133.8$ (q, carbodiimide), 95.2, (q, Fc), 66.3 ppm (CH, Fc); IR (CH_2Cl_2): $\tilde{\nu}_{max}$ = 2952, 2919, 2190, 2138, 1512, 1452, 1302, 1243, 1174, 1115, 1029, 810, 723 cm^{-1}; MS (70 eV, EI): *m*/*z* (%): 448 (100) [M^+], 370 (6), 277 (85), 268 (19), 242 (14); elemental analysis calcd (%) for $C_{22}H_{16}Fe_2N_4$ (448): C 58.97, H 3.60, N 12.50; found: C 58.81, H 3.49, N 12.59.

General procedure for the preparation of [3,3]ferrocenophanes 4–7: A solution of the appropriate amine (0.892 mmol) in the same solvent (20 mL) was added dropwise to a solution of 1,3,10,12-tetraaza-[3,3]ferrocenophane (**3**; 0.1 g, 0.223 mmol) in dry THF (15 mL) at room temperature and under a nitrogen atmosphere. After the mixture was stirred for 3 h at room temperature the solvent was removed by rotary evaporation and the residue was triturated with *n*-hexane/diethyl ether (1:1) to give a pale yellow solid which was crystallized from CH_2Cl_2/Et_2O (2:1).

Compound 4: 77 %; m.p. 194–197 °C (decomp); ^{1}H NMR (200 MHz, [D$_6$]DMSO, 25 °C, TMS): $\delta = 8.20$ (s, 2H; NH), 7.09–7.15 (m, 8H; Ar), 4.94 (brt, 2H; NH), 4.17 (s, 4H; CH_2), 4.14 (s, 1H; NH), 3.98 (brs, 8H; Fc), 3.93 (brs, 8H; Fc), 2.24 ppm (brs, 6H; CH_3); ^{13}C NMR (50 MHz, [D$_6$]DMSO, 25 °C, TMS): $\delta = 150.4$ (q, guanidine), 137.4 (q, Ar), 135.6 (q, Ar), 128.8 (CH, Ar), 127.2 (CH, Ar), 64.7 (CH, Fc), 63.6 (CH, Fc), 62.0 (CH, Fc), 39.9 (CH_2), 20.7 ppm (CH_3); IR (Nujol): $\tilde{\nu}_{max}$ = 3420, 3243, 3164, 1624, 1593, 1567, 1506, 1313, 1240, 1180, 1018, 906, 800 cm^{-1}; MS (FAB$^+$), *m*/*z* (%): 691 (100) [M^++1]; elemental analysis calcd (%) for $C_{38}H_{38}Fe_2N_6$ (690): C 66.09, H 5.51, N 12.17; found: C 65.98, H 5.43, N 12.29.

Compound 5: 75 %; m.p. 211–214 °C (decomp); ^{1}H NMR (400 MHz, [D$_6$]DMSO, 25 °C, TMS): $\delta = 8.26$ (s, 1H; NH), 8.05 (d, ^3J(H,H) = 6.8 Hz, 2H; Ar), 7.90 (d, ^3J(H,H) = 8.3 Hz, 2H; Ar), 7.80 (d, ^3J(H,H) = 6.3 Hz, 2H; Ar), 7.44–7.55 (m, 8H; Ar), 5.06 (brt, 2H; NH), 4.72 (d, ^3J(H,H) = 4.6 Hz, 4H; CH_2), 4.19 (s, 1H; NH), 3.98 (brs, 8H; Fc), 3.91 ppm (brs, 8H; Fc); ^{13}C NMR (100 MHz, [D$_6$]DMSO, 25 °C, TMS): $\delta = 150.3$ (q, guanidine), 135.5 (q, Ar), 133.3 (q, Ar), 130.8 (q, Ar), 128.2 (CH, Ar), 127.0 (CH, Ar), 125.7 (CH, Ar), 125.4 (CH, Ar), 125.2 (CH, Ar), 124.6 (CH, Ar), 123.4 (CH, Ar), 64.4 (CH, Fc), 63.4 (CH, Fc), 61.7 (CH, Fc), 42.5 ppm (CH_2); IR (Nujol): $\tilde{\nu}_{max}$ = 3406, 3269, 1619, 1590, 1554, 1531, 1307, 1143, 1024, 819 cm^{-1}; MS (FAB$^+$): *m*/*z* (%): 763 (100) [M^++1]; elemental analysis calcd (%) for $C_{44}H_{38}Fe_2N_6$ (762): C 69.29, H 4.99, N 11.02; found: C 69.15, H 4.84, N 11.21.

Compound 6: 82 %; m.p: 198–202 °C (decomp); ^{1}H NMR (400 MHz, [D$_6$]DMSO, 25 °C, TMS): $\delta = 8.77$ (s, 2H; Ar), 8.64 (s, 1H; NH), 8.30 (s, 1H; NH), 8.16 (s, 1H; NH), 8.08 (m, 3H; Ar and NH), 7.23 (s, 1H; NH), 6.50 (brs, 2H; Ar), 5.09 (s, 1H; NH), 4.90 (s, 1H; NH), 3.77–4.37 (m, 16H; Fc), 3.44 (brt, 4H; CH_2), 3.24 ppm (brt, 4H; CH_2); ^{13}C NMR (100 MHz, [D$_6$]DMSO, 25 °C, TMS): $\delta = 161.5$ (q, Ar), 150.6, (q, guanidine), 148.8 (CH, Ar), 134.1 (CH, Ar), 131.7 (q, Ar), 108.3 (CH, Ar), 64.4 (CH, Fc), 63.5 (CH, Fc), 61.6 (CH, Fc), 41.0 ppm (2×CH_2); IR (Nujol): $\tilde{\nu}_{max}$ = 3428, 3397, 3277, 1604, 1551, 1526, 1331, 1290, 1119, 1038, 807 cm^{-1}; MS (FAB$^+$): *m*/*z* (%): 813 (100) [M^++1]; elemental analysis calcd (%) for $C_{36}H_{36}Fe_2N_{10}O_4$ (812): C 53.20, H 4.43, N 20.69; found: C 52.94, H 4.47, N 20.74.

Compound 7: 70 %; m.p: 144–147 °C; ^{1}H NMR (600 MHz, [D$_6$]DMSO, 65 °C, TMS): $\delta = 8.43$ (s, 1H; NH), 4.58 (brs, 2H; NH), 4.14 (brs, 4H; CH_2), 4.12 (t, ^3J(H,H) = 1.8 Hz, 6H; Fc), 4.09 (t, ^3J(H,H) = 1.8 Hz, 6H; Fc), 4.06 (brs, 8H; Fc), 4.04 (s, 10H; Fc), 3.93 ppm (brs, 4H; Fc); ^{13}C NMR (75.3 MHz, [D$_6$]DMSO, 25 °C, TMS): $\delta = 152.1$ (q, guanidine), 91.4 (q, Fc), 86.7 (q, Fc), 68.2 (CH, Fc), 68.1 (CH, Fc), 67.7 (CH, Fc), 67.0 (CH, Fc), 64.9 (CH, Fc), 63.8 (CH, Fc), 62.1 (CH, Fc), 40.5 ppm (CH_2); IR (Nujol): $\tilde{\nu}_{max}$ = 3418, 3260, 3092, 1622, 1568, 1400, 1313, 1253, 1188, 1118, 1026, 819 cm^{-1}; MS (FAB$^+$): *m*/*z* (%): 879 (48) [M^++1]; elemental analysis calcd (%) for $C_{44}H_{42}Fe_2N_6$ (878): C 60.14, H 4.78, N 9.57; found: C 59.92, H 4.75, N 9.76.

X-ray data for compound 7: Orange prism, 0.20×0.18×0.12 mm size, triclinic, P$\bar{1}$, $a = 11.963(2)$, $b = 13.176(3)$, $c = 13.849(3)$ Å, $\alpha = 93.54(3)$, $\beta = 91.56(3)$, $\gamma = 114.74(3)$, $V = 1975.3(9)$ Å^3, $Z = 2$, $\rho_{calcd} = 1.608$ g cm^{-3}, $\theta_{max} = 27.97$, $Mo_{K\alpha}$, $\lambda = 0.71073$ Å, ω-scan, diffractometer Siemens SMART APEX, $T = 100(2)$ K, 21913 reflections collected, of which 8023 were independent ($R_{int} = 0.026$), absorption correction based on multiscans, T_{min}/T_{max} 0.748/0.837, direct primary solution and refinement on F^2 (SHELXS-97 and SHELXL-97, G. M. Sheldrick, University of Göttingen, **1997**), 541 refined parameters, N–H hydrogen atoms refined as free, rigid methyl groups, others as riding. $R_1[I > 2\sigma(I)] = 0.0559$, wR_2(all data) = 0.1281.

CCDC-629230 contains the supplementary crystallographic data for this paper. These data can be obtained free of charge from The Cambridge Crystallographic Data Centre via www.ccdc.cam.ac.uk/data_request/cif.

Acknowledgements

We gratefully acknowledge the grants from MEC-Spain (CTQ2004—02201) and from Fundación Séneca (CARM) (02970/PI/05).

[1] For a review see: G. J. Kirkovits, J. A. Shriver, P. A. Gale, J. L. Sessler, *J. Inclusion Phenom. Macrocycl. Chem.* **2001**, *41*, 69–75. For recent references see: a) M. J. Mahoney, A. M. Beatty, B. D. Smith, *J. Am. Chem. Soc.* **2001**, *123*, 5847–5848; b) H. Miyaji, S. R. Collison, I. Prokés, J. H. R. Tucker, *Chem. Commun.* **2003**, 64–65; c) F. Otón, A. Tárraga, M. D. Velasco, P. Molina, *Dalton Trans.* **2005**, 1159–1161; d) C. Suksai, P. Leeladee, D. Jainuknan, T. Tuntulani, N. Muangsin, O. Chailapakul, P. Kongsaeree, C. Pakavatchai, *Tetrahedron Lett.* **2005**, *46*, 2765–2769; e) F. Otón, A. Tárraga, A. Espinosa, M. D. Velasco, P. Molina, *Dalton Trans.* **2006**, 3685–3692.

[2] C. L. Hannon, E. V. Anslyn in *Bioorganic Chemistry Frontiers, Vol. 3* (Eds.: H. Duggas, F. P. Schmidtchen), Springer, Berlin, **1993**, pp. 193–255.

[3] a) M. D. Best, S. L. Tobey, E. V. Anslyn, *Coord. Chem. Rev.* **2003**, *240*, 3–15; b) G. Müller, J. Riede, F. P. Schmidtchen, *Angew. Chem.* **1988**, *100*, 1574–1575; *Angew. Chem. Int. Ed. Engl.* **1988**, *27*, 1516–1518; c) K. A. Schug, W. Lindner, *Chem. Rev.* **2005**, *105*, 67–113; d) C. Seel, A. Galan, J. de Mendoza, *Top. Curr. Chem.* **1995**, *175*, 101–132; e) M. Berger, F. P. Schmidtchen, *Chem. Rev.* **1997**, *97*, 1609–1646; f) B. P. Orner, A. D. Hamilton, *J. Incl. Phenom. Macrocycl. Chem.* **2001**, *41*, 141–147; g) R. J. T. Houk, S. L. Tobey, E. V. Anslyn, *Top. Curr. Chem.* **2005**, *255*, 199–229.

[4] P. J. Baily, S. Pace, *Coord. Chem. Rev.* **2001**, *214*, 91–141.

[5] M. P. Coles, *Dalton Trans.* **2006**, 985–1001.

[6] a) E. M. A. Ratilla, N. M. Kostic, *J. Am. Chem. Soc.* **1998**, *120*, 4427–4428; b) E. M. A. Ratilla, B. K. Scott, M. S. Moxness, N. M. Kostic, *Inorg. Chem.* **1990**, *29*, 918–926; c) S. Aioki, K. Iwaida, N. Hanamoto, M. Shiro, E. Kimura, *J. Am. Chem. Soc.* **2002**, *124*, 5256–5257.

[7] For a review, see: a) P. D. Beer, P. A. Gale, Z. Chen, *Coord. Chem. Rev.* **1999**, *185–186*, 3–36. For recent examples, see: b) J. L. López, A. Tárraga, A. Espinosa, M. D. Velasco, P. Molina, V. Lloveras, J. Vidal-Gancedo, C. Rovira, J. Veciana, D. J. Evans, K. Wurst, *Chem. Eur. J.* **2004**, *10*, 1815–1826; c) A. Caballero, V. Lloveras, A. Tárraga, A. Espinosa, M. D. Velasco, J. Vidal-Gancedo, C. Rovira, K. Wurst, P. Molina, J. Veciana, *Angew. Chem.* **2005**, *117*, 2013–2017; *Angew. Chem. Int. Ed.* **2005**, *44*, 1977–1981; d) A. Caballero, R. Martinez, V. Lloveras, I. Ratera, J. Vidal-Gancedo, K. Wurst, A. Tárraga, P. Molina, J. Veciana, *J. Am. Chem. Soc.* **2005**, *127*, 15666–15667; e) A. Caballero, A. Tárraga, M. D. Velasco, P. Molina, *Dalton Trans.* **2006**, 1390–1398.

[8] For reviews, see: a) P. D. Beer, P. A. Gale, *Angew. Chem.* **2001**, *113*, 502–532; *Angew. Chem. Int. Ed.* **2001**, *40*, 486–516; b) P. A. Gale, *Coord. Chem. Rev.* **2000**, *199*, 181–233; c) P. A. Gale, *Coord. Chem. Rev.* **2001**, *213*, 79–128. For recent examples, see: d) F. Otón, A. Tárraga, M. D. Velasco, A. Espinosa, P. Molina, *Chem. Commun.* **2004**, 1658–1659; e) F. Otón, A. Tárraga, A. Espinosa, M. D. Velasco, D. Bautista, P. Molina, *J. Org. Chem.* **2005**, *70*, 6603–6608; f) F. Otón, A. Tárraga, A. Espinosa, M. D. Velasco, P. Molina, *J. Org. Chem.* **2006**, *71*, 4590–4598.

[9] J. Westwood, S. J. Coles, S. R. Collison, G. Gasser, S. J. Green, M. B. Hursthouse, M. E. Light, J. H. R. Tucker, *Organometallics* **2004**, *23*, 946–951, and references therein.

[10] a) P. D. Beer, M. G. B. Drew, D. K. Smith, *J. Organomet. Chem.* **1997**, *543*, 259–261; b) Preliminary communication of this work: F. Otón, A. Tarraga, P. Molina, *Org. Lett.* **2006**, *8*, 2107–2110.

[11] a) P. Molina, M. J. Vilaplana, *Synthesis* **1994**, 1197–1218; b) P. M. Fresneda, P. Molina, *Synlett* **2004**, 1–17.

[12] A. Arques, P. Molina, *Current Org. Chem.* **2004**, *8*, 827–843.

[13] The synthesis of 1,1′-diazidoferrocene has been previously described by reaction of 1,1′-dilithioferrocene with 1,1,2,2-tetrabromoethane and subsequent halide displacement by using NaN_3/CuCl: A. Shafir, M. P. Power, G. D. Whitener, J. Arnold, *Organometallic*s **2000**, *19*, 3978–3982.

[14] P. Petrovitch, *Double Liaison* **1966**, *133*, 1093–1109.

[15] A. Tárraga, F. Otón, A. Espinosa, M. D. Velasco, P. Molina, D. J. Evans, *Chem. Commun.* **2004**, 458–459.

[16] D. E. Bublitz, *J. Organomet. Chem.* **1970**, *23*, 225–228.

[17] The DPV technique has been employed to obtain well-resolved potential information, because the individual redox processes are poorly resolved in the CV experiments, the individual $E_{1/2}$ potentials cannot easily be extracted from this data accurately. See: B. R. Serr, K. A. Andersen, C. M. Elliot, O. P. Anderson, *Inorg. Chem.* **1988**, *27*, 4499–4504.

[18] a) P. D. Beer, A. R. Graydon, A. O. M. Johnson, D. K. Smith, *Inorg. Chem.* **1997**, *36*, 2112–2118; b) H. Miyaji, G. Gasser, S. J. Green, Y. Molard, S. M. Strawbridge, J. H. R. Tucker, *Chem. Commun.* **2005**, 5355–5357.

[19] J. L. Sessler, E. Katayev, G. Dan Pantos, Y. A. Ustynyuk, *Chem. Commun.* **2004**, 1276–1277.

[20] P. Debroy, M. Baberjee, M. Prasad, S. P. Moulik, S. Roy, *Org. Lett.* **2005**, *7*, 403–406.

[21] M. J. Haynes, *J. Chem. Soc. Dalton Trans.* **1993**, 311–312.

[22] a) F. P. Schmidtchen, *Org. Lett.* **2002**, *4*, 431–434; b) S. L. Tobey, E. V. Anslyn, *J. Am. Chem. Soc.* **2003**, *125*, 14807–14815; c) C.-H. Lee, D.-D. Na, D.-W. Yoon, D.-H. Won, W. S. Cho, V. M. Lynch, S. V. Shevchuk, J. L. Sessler, *J. Am. Chem. Soc.* **2003**, *125*, 7301–7306; d) M. R. Sambrook, P. D. Beer, R. L. Wisner, R. L. Paul, A. R. Cowly, F. Szemes, M. G. B. Drew, *J. Am. Chem. Soc.* **2005**, *127*, 2292–2302; e) J. L. Sessler, D. An, W.-S. Cho, V. M. Lynch, M. Marquez, *Chem. Eur. J.* **2005**, *11*, 2001–2011.

[23] T. Farrel, T. Meyer-Friedrichsen, M. Malessa, D. Haase, W. Saak, I. Asselberghs, K. Wostyn, K. Clays, A. Persoons, J. Heck, A. R. Manning, *J. Chem. Soc. Dalton Trans.* **2002**, 29–36, and references therein.

[24] a) G. L. Geoffroy, M. S. Wrighton, *Organometallic Photochemistry*, Academic Press, New York, **1979**; b) Y. S. Sohn, D. N. Hendrickson, H. B. Gray, *J. Am. Chem. Soc.* **1971**, *93*, 3603–3612.

[25] S. Barlow, H. E. Bunting, C. Ringham, J. C. Green, G. U. Bublitz, S. G. Boxer, J. W. Perry, S. R. Marder, *J. Am. Chem. Soc.* **1999**, *121*, 3715–3723.

[26] a) S. R. Marder, J. W. Perry, B. G. Tiemann, *Organometallics*, **1991**, *10*, 1896–1901; b) B. J. Coe, C. J. Jones, J. A. McCleverty, D. Bloor, G. J. Cross, *J. Organomet. Chem.* **1994**, *464*, 225–232; c) T. J. Müller, A. Netz, M. Ansorge, *Organometallics* **1999**, *18*, 5066–5074.

[27] Specfit/32 Global Analysis System, **1999–2004**, Spectrum Software Associates (SpectSoft@compuserve.com).

[28] S. Fery-Forgues, B. Delavaux-Nicot, *J. Photochem. Photobiol. A* **2000**, *132*, 137–159.

[29] For a recent example see: R. Martinez, I. Ratera, A. Tarraga, P. Molina, J. Veciana, *Chem. Commun.* **2006**, 3809–3811.

[30] D. E. Richarson, H. Taube, *Inorg. Chem.* **1981**, *20*, 1278–1285.

[31] F. Barriere, N. Camire, W. E. Geiger, U. T. Mueller-Weaterhoff, R. Sanders, *J. Am. Chem. Soc.* **2002**, *124*, 7262–7263.

[32] S. Barlow, D. O'Hare, *Chem. Rev.* **1997**, *97*, 637–669.

[33] N. S. Hush, *Prog. Inorg. Chem.* **1967**, *8*, 391–444.

[34] C. Creutz, *Prog. Inorg. Chem.* **1983**, *30*, 1–73.

[35] B. S. Brunschwig, C. Creutz, N. Sutin, *Chem. Soc. Rev.* **2002**, *31*, 168–184.

[36] C. Levanda, K. Bechgaard, D. O. Cowan, *J. Org. Chem.* **1976**, *41*, 2700–2704.

[37] K. H. H. Fabian, H.-J. Lindner, N. Nimmerfroh, K. Hafner, *Angew. Chem.* **2001**, *113*, 3517–3520; *Angew. Chem. Int. Ed.* **2001**, *40*, 3402–3405; .

[38] Gaussian 03 (Revision B.03), M. J. Frisch, G. W. Trucks, H. B. Schlegel, G. E. Scuseria, M. A. Robb, J. R. Cheeseman, J. A. Montgomery, Jr., T. Vreven, K. N. Kudin, J. C. Burant, J. M. Millam, S. S. Iyengar, J. Tomasi, V. Barone, B. Mennucci, M. Cossi, G. Scalmani, N. Rega, G. A. Petersson, H. Nakatsuji, M. Hada, M. Ehara, K. Toyota, R. Fukuda, J. Hasegawa, M. Ishida, T. Nakajima, Y. Honda, O. Kitao, H. Nakai, M. Klene, X. Li, J. E. Knox, H. P. Hratchian, J. B. Cross, V. Bakken, C. Adamo, J. Jaramillo, R. Gomperts, R. E. Stratmann, O. Yazyev, A. J. Austin, R. Cammi, C. Pomelli, J. W. Ochterski, P. Y. Ayala, K. Morokuma, G. A. Voth, P. Salvador, J. J. Dannenberg, V. G. Zakrzewski, S. Dapprich, A. D. Daniels, M. C. Strain, O. Farkas, D. K. Malick, A. D. Rabuck, K. Raghavachari, J. B. Foresman, J. V. Ortiz, Q. Cui, A. G. Baboul, S. Clifford, J. Cioslowski, B. B. Stefanov, G. Liu, A. Liashenko, P. Piskorz, I. Komaromi, R. L. Martin, D. J. Fox, T. Keith, M. A. Al-Laham, C. Y. Peng, A. Nanayakkara, M. Challacombe, P. M. W. Gill, B. Johnson, W. Chen, M. W. Wong, C. Gonzalez, J. A. Pople, Gaussian Inc., Wallingford, CT, **2004**.

[39] L. J. Bartolottiand, K. Fluchick in *Reviews in Computational Chemistry, Vol. 7* (Eds.: K. B. Lipkowitz, B. D. Boyd), VCH, New York, **1996**, pp. 187–216.

[40] a) S. Miertus, E. Scrocco, J. Tomasi, *Chem. Phys.* **1981**, *55*, 117–129; b) R. Cammi, B. Mennucci, J. Tomasi, *J. Phys. Chem. A* **2000**, *104*, 5631–5637; c) M. Cossi, N. Rega, G. Scalmani, V. Barone, *J. Comput. Chem.* **2003**, *24*, 669–681.

Received: December 7, 2006
Revised: January 21, 2007
Published online: April 20, 2007

